A Mean Field Game for Capacity Expansion Modeling

Emma Hubert*† Dimitrios Lolas* Ronnie Sircar*

10 July, 2025

Abstract

This paper studies the optimal investment behavior of renewable electricity producers in a competitive market, where both prices and installation costs are influenced by aggregate industry activity. We model the resulting crowding effects using a mean field game framework, capturing the strategic interactions among a continuum of heterogeneous producers. The equilibrium dynamics are characterized via a coupled system of Hamilton–Jacobi–Bellman and Fokker–Planck equations, which describe the value function of a representative producer and the evolution of the distribution of installed capacities over time. We analyze both deterministic and stochastic versions of the model, providing analytical insights in tractable cases and developing numerical methods to approximate the general solution. Simulation results illustrate how aggregate investment responds to changing market conditions, cost structures, and exogenous productivity shocks.

Keywords. Mean field games, optimal control, renewable investments.

AMS 2020 subject classifications. 91A16; 49L12; 91B74.

1 Introduction

As nations accelerate their transition towards low-carbon economies, the expansion of renewable energy sources, particularly solar and wind, has become a critical priority. However, this shift also brings substantial new challenges for electricity systems. A striking illustration occurred in April 2025, when much of Spain and parts of Portugal experienced a massive power outage affecting millions of households (see, for instance Bajo-Buenestado (2025) [6]). Although investigations are ongoing at time of writing, the incident highlights how increasing reliance on weather-dependent generation can amplify vulnerabilities to unexpected disturbances. More broadly, the growing prevalence of negative electricity prices in countries with deep renewables penetration further exemplifies the economic and operational stresses induced by this transition.

*Department of Operations Research & Financial Engineering, Princeton University.

†Research partially supported by the NSF grant DMS-2307736.

These phenomena underline the urgent need for careful planning of capacity expansion, not only to meet decarbonization targets but also to ensure system resilience. A variety of complementary solutions have been explored, such as demand-side response programs, investments in grid-scale storage, reinforcement of transmission networks, and dynamic pricing mechanisms. Yet, long-term investment decisions by competing firms remain central to the evolution of electricity markets, shaping both the pace and the stability of renewables integration. Capacity expansion planning must therefore balance the twin goals of promoting rapid deployment and preserving economic and operational robustness. In this context, mathematical modeling—including dynamic games, mean-field approximations, and stochastic control approaches—plays a crucial role in understanding strategic interactions between firms and guiding the design of efficient policy interventions (see for example Cacciarelli, Pinson, Panagiotopoulos, Dixon, and Blaxland (2025) [9]).

When modeling investment decisions in general, and in particular in energy systems, a common approach is to formulate dynamic control or stopping problems, often under uncertainty. In such frameworks, a central planner or a representative agent optimizes a long-term objective, accounting for evolving technological, market, and regulatory conditions (see, for example, Aïd, Campi, Nguyen Huu, and Touzi (2009) [1], Carmona and Ludkovski (2010) [10], Ludkovski and Sircar (2016) [27]). However, when considering renewable energy installations, such as solar panels which can be deployed relatively easily and at varying scales by a multitude of actors, it becomes essential to explicitly model the decentralized and competitive nature of investment. The price of electricity, which depends on the aggregate level of installed capacity, becomes a key channel of interaction between these agents. Directly analyzing multi-player dynamic games, however, quickly leads to computational intractability as the number of participants grows. To overcome this difficulty, it is common to study the limiting regime where the number of players tends to infinity, leading to more tractable mean field approximations that capture the aggregate effect of individual behaviors.

Mean field games (MFGs) study the limiting behaviour of stochastic differential games as the number of (exchangeable) players tends to infinity (see, for instance, Guéant, Lasry, and Lions (2011) [24] for an early review article). In this framework, each agent optimizes their objective function, taking as given the aggregate behavior of the population, which is itself determined in equilibrium as a fixed point of the collective dynamics of the individual strategies. The MFG formulation has since been widely adopted to analyze decentralized decision-making in large populations, providing both analytical and numerical tractability, and insight into emergent macro-level behavior.

In recent years, MFGs have been increasingly applied to a wide range of problems in energy systems. These include renewable investment decisions by Aïd, Dumitrescu, and Tankov (2021) [2], Alasseur, Basei, Bertucci, and Cecchin (2023) [5], Escribe, Garnier, and Gobet (2024) [20] or Aïd, Federico, Ferrari, and Rodosthenous (2025) [3], electricity storage optimization by Alasseur, Ben Taher, and Matoussi (2020) [4], and the design of demand-response programs by Élie, Hubert, Mastrolia, and Possamaï (2021) [19]. MFGs have also been used to study energy mix transitions by Chan and Sircar (2017) [15] and carbon emissions regulation by Carmona, Dayanıklı, and Laurière (2022) [13], Hernández Santibáñez,

Jofré, and Possamaï (2023) [25], Bichuch, Dayanıklı, and Lauriere (2024) [8], Dayanikli and Laurière (2024) [16], as well as market design and electricity price formation by Firoozi, Shrivats, and Jaimungal (2022) [21] or Bassière, Dumitrescu, and Tankov (2024) [7]. More recently, the framework has been extended to analyze broader aspects of the energy transition, by Dumitrescu, Leutscher, and Tankov (2024) [18], and energy expenditure from cryptocurrency mining by Li, Reppen, and Sircar (2024) [26]. This list is far from exhaustive, but illustrates the growing role of MFGs in understanding the complex dynamics of modern energy systems.

Among the aforementioned papers, we motivate our work from [5], which develops a deterministic mean-field-type model for capacity expansion in solar energy with an infinite time horizon. In this model, identical producers optimize solar production capacity, and interact through the electricity price, which depends of the total installed capacity. This framework captures the trade-off between investment rewards, costs and the price-depressing effects of overcapacity. This paper characterizes the steady-state equilibrium using Pontryagin's maximum principle, and provides a study of the effects of subsidies for solar production from a central planner's point of view.

The model we propose can be seen as a finite-horizon reformulation of [5], with two key extensions. First, we allow for heterogeneity in initial capacities across producers. This extension is particularly relevant in the context of solar energy, where small-scale residential investors may compete with large-scale solar farms. Second, we include interaction not only through the state (installed capacity) but also through the control (installation rate), introducing a crowding effect. Indeed, while producers naturally interact through the market price of electricity, which depends on total installed capacity, installation costs may also be influenced by the aggregate speed of investment across the market, for instance, due to supply-chain congestion or labor constraints.

We employ an approximation where aggregates (or sums) are replaced by a continuum mean multiplied by the number of agents in the sum. This has been used in models of cryptocurrency mining in [26] and Garcia, Sircar, and Soner (2025) [23], and its error is analyzed in Garcia, Reppen, and Sircar (2025) [22]. It allows finite agent games with interaction through aggregates to benefit from mean field game technology, in particular reduction of dimension. In the current model, the aforementioned features lead naturally to a mean field game of both state and control, allowing us to study dynamic investment behavior, threshold effects, and the evolution of aggregate capacity over time.

Finally, unlike [5], we consider a finite time horizon, which better reflects the long but bounded planning horizons of investors in the energy sector. For example, investors may anticipate changes in technology or policy over the next two or three decades, such as the emergence of alternative energy sources or regulatory shifts, and may thus optimize over a finite investment window. Nevertheless, the approach we develop here could be naturally reduced to the infinite-horizon setting.

Our analysis is based on characterizing the mean field game equilibrium via a system of coupled Hamilton–Jacobi–Bellman (HJB) and Fokker–Planck (FP) equations. In an homogeneous setting, where all producers start with the same initial capacity, our model reduces

to a deterministic control problem similar to [5], but with a finite-time horizon, for which we prove existence and uniqueness of solutions to a forward-backward ODE system and identify threshold behavior in optimal investment. In the heterogeneous case, we study the full mean field game of state and control, establish the structure of the equilibrium using partial differential equation (PDE) methods, and analyze the resulting distribution of installed capacities. In the case of a linear price function, we propose a numerical method based on a quadratic ansatz in the non-installation region and a finite difference scheme in the installation region. We also extend the model to include idiosyncratic randomness in the capacity dynamics, showing that our framework remains tractable under stochastic perturbations.

The remainder of the paper is organized as follows. In Section 2, we introduce our model and its main features. In Section 3, we analyze the homogeneous agents case and derive explicit characterizations of the equilibrium. In Section 4, we turn to the heterogeneous setting, study the associated HJB–FP system, and present our numerical scheme. Finally, in Section 5, we show how our framework extends to include randomness in capacity dynamics. We conclude in Section 6 with a discussion of extensions and policy implications.

2 Model formulation

The formulation of our model echoes that of [5], but is adapted to a finite time horizon $T > 0$ (in years) and designed to account for potential heterogeneity in the initial capacities of investors.

We first consider the finite-player model with $N + 1$ renewable producers, indexed by $i \in \{0, \dots, N\}$. Each producer is characterized by their installed capacity $x_t^{(i)}$ in MW at time $t \in [0, T]$. In the absence of new investment, installed capacity is assumed to depreciate exponentially at rate $\delta > 0$, reflecting a gradual loss in production efficiency over time. A producer $i \in \{0, \dots, N\}$ can invest in new capacity by choosing an installation rate $\nu_t^{(i)} \geq 0$ at each time $t \in [0, T]$, which represents the rate in MW/year at which new capacity is added. The dynamics of installed capacity for producer i then follow:

$$\mathrm{d}x_t^{(i)} = (-\delta x_t^{(i)} + \nu_t^{(i)})\,\mathrm{d}t, \quad \text{for } t \in [0, T], \tag{1}$$

starting from a fixed initial installed capacity $x_0^{(i)} \geq 0$, and where $\delta > 0$ is the depreciation rate as above. The total (or aggregate) installed capacity is denoted by

$$X_t := \sum_{j=0}^{N} x_t^{(j)}, \quad t \in [0, T]. \tag{2}$$

Note that since the installation rate is assumed to be non-negative, we necessarily have

$$X_t \geq \mathrm{e}^{-\delta t} \sum_{j=0}^{N} x_0^{(j)}, \quad t \in [0, T]. \tag{3}$$

The aggregate installed capacity impacts the price at which all producers sell electricity. More precisely, we assume that the common market price at time t is given by $P(\lambda_t X_t)$

(in \$/MWh), for a (strictly) decreasing price function $P : \mathbb{R}_+ \longrightarrow \mathbb{R}$, reflecting the idea that higher total capacity depresses the market price of electricity due to an abundance of cheap renewable production. The parameter λ_t represents the fraction of installed capacity that is effectively producing electricity at time t, and thus accounts for the intermittency of renewable energy sources, such as variability in wind or sunlight. For simplicity, we assume $\lambda_t \equiv \lambda \in (0, 1]$ is constant over time and we absorb this constant to P.

Following [5], the marginal cost of production is constant, denoted by $c > 0$ (in \$/MWh), and represents operational expenses associated with running the installed capacity. This may include maintenance, insurance and other ongoing management costs of operating a renewable energy asset such as a solar or wind installation. We also model the cost of installing new capacity through two distinct mechanisms that curb rapid expansion:

- (i) $\alpha > 0$ (in \$/MW) is the marginal installation cost;
- (ii) $\beta > 0$ (in (\$ year)/MW^2) is a crowding sensitivity parameter, capturing the additional cost per MW of capacity that arises from increased installation activity in the market. This reflects market frictions such as limited contractor availability, supply chain bottlenecks, or permitting delays that become more pronounced when many producers are simultaneously expanding.

However, contrary to [5], we assume that the installation cost is not constant, but instead increases with the total installation rate due to crowding effects. More precisely, the instantaneous cost of installing new capacity $\nu_t^{(i)}$ is defined as follows:

$$\nu_t^{(i)}(\alpha + \beta K_t), \quad \text{with} \quad K_t \coloneqq \sum_{j=0}^{N} \nu_t^{(j)}, \quad t \in [0, T]. \tag{4}$$

Finally, given a fixed initial installed capacity $x_0^{(i)} \geq 0$, the individual producer's objective is defined by the following maximization problem

$$J_i(x_0^{(i)}) := \sup_{\nu^{(i)} \geq 0} \int_0^T \mathrm{e}^{-rt} \Big((P(X_t) - c) h x_t^{(i)} - \alpha \nu_t^{(i)} - \beta \nu_t^{(i)} K_t \Big) \mathrm{d}t, \tag{5}$$

where $h \in [0,\, 8760]$ is the number of production hours per year, and $r > 0$ is a discount rate.

As is well known, this type of multi-agent non-zero sum differential game is difficult to solve, even for the two-player case. For analytical and computational tractability, we will instead study a continuum approximation by a type of mean field game, where a continuum mean multiplied by the number of players proxies for the aggregate quantities X and K, respectively defined in (2), (4). We first consider in the next section the simpler case of homogeneous producers; the study of the general mean field game is postponed to Section 4.

3 Homogeneous producers

In this section, we assume that all producers start with the same initial installed capacity, $x_0^{(i)} =: x_0 \geq 0$ for all $i \in \{0, \ldots, N\}$. This simplification, which makes our model a finite-horizon counterpart of [5] and thus facilitates comparison, will be relaxed in the next section.

In this setting, producers are indistinguishable, and their optimal actions can be derived using Pontryagin's maximum principle, as in [5].

More precisely, we first focus on the ith producer's optimization problem, $i \in \{0, \dots, N\}$, for fixed capacity and effort of other producers. The Hamiltonian corresponding to the objective function (5) is given by

$$H_t^{(i)}(x_t^{(i)}, u_t^{(i)}, \nu_t^{(i)}) \coloneqq u_t^{(i)}(-\delta x_t^{(i)} + \nu_t^{(i)}) + (P(X_t) - c)hx_t^{(i)} - \alpha\nu_t^{(i)} - \beta\nu_t^{(i)}K_t, \quad t \in [0, T],$$

where $u^{(i)}$ is the adjoint variable, or costate. Recalling that K defined in (4) depends on $\nu^{(i)}$, the maximization of the previous Hamiltonian leads to the following installation rate

$$\nu_t^{(i)} = \frac{1}{2\beta}\left(u_t^{(i)} - \alpha - \beta\sum_{j\neq i}\nu_t^{(j)}\right)^+, \quad t \in [0, T].$$

Under the assumption of homogeneous producers, all adjoint variables $u^{(i)}$, $i \in \{0, \dots, N\}$, actually coincide, as well as the corresponding optimal investment rates, which can thus be derived by solving the previous equation, leading to

$$\nu_t^{(i)} = \frac{1}{\beta(N+2)}(u_t^{(i)} - \alpha)^+, \quad t \in [0, T].$$

Furthermore, the costate $u^{(i)}$ satisfies the following ordinary differential equation (ODE):

$$\dot{u}_t^{(i)} = (r + \delta)u_t^{(i)} - (P(X_t) - c)\, h - hx_t^{(i)}\frac{\partial P(X_t)}{\partial x_t^{(i)}}, \quad t \in [0, T], \quad u_T^{(i)} = 0.$$

We will subsequently drop the dependence on the index i, since all producers are identical.

As the number of producers is assumed to be large, we follow here the standard mean field game convention by assuming that the impact of an individual producer to the total capacity is negligible, *i.e.*

$$\frac{\partial P(X_t)}{\partial x_t^{(i)}} \approx 0.$$

Replacing in the above ODE for the costate, we derive the following simplified ODE,

$$\dot{u}_t = (r + \delta)u_t - (P(X_t) - c)h, \quad t \in [0, T], \quad u_T = 0.$$

Still under the assumption that N is large, the natural approximation $\frac{N+1}{N+2} \approx 1$ leads to the following formula for the total installation rate defined in (4),

$$K_t \coloneqq \sum_{j=0}^{N}\nu_t^{(j)} = \frac{1}{\beta}(u_t - \alpha)^+,$$

highlighting in particular that installation of new capacity occurs at time $t \in [0, T]$ if and only if $u_t > \alpha$. Finally, summing (1) over $i \in \{0, \dots, N\}$ and using the previous equation, we derive the following ODE for the total installed capacity defined in (2),

$$\dot{X}_t + \delta X_t = \frac{1}{\beta}(u_t - \alpha)^+, \quad t \in [0, T], \quad X_0 = (N + 1)x_0.$$

In summary, when N is sufficiently large, the original multi-player non-zero-sum game with homogeneous producers can be asymptotically approximated by a mean field game, characterized by the following forward-backward system:

$$\dot{X}_t = -\delta X_t + \frac{1}{\beta}(u_t - \alpha)^+, \qquad t \in [0,T], \quad X_0 = (N+1)x, \tag{6a}$$

$$\dot{u}_t = (r+\delta)u_t - (P(X_t) - c)\, h, \quad t \in [0,T], \quad u_T = 0. \tag{6b}$$

The previous system is the finite-horizon analogue of the one derived in [5]. In the next section, we first prove existence and uniqueness for the system (6a)–(6b) under some regularity assumptions for the price function P. We then highlight some interesting properties of the solution and the associated optimal installation rate. These theoretical results offer preliminary insights into the investment problem, which are further developed and illustrated by the numerical simulations presented at the end of this section.

3.1 Theoretical results

As mentioned above, the first main result establishes existence and uniqueness of the forward-backward system (6a)–(6b).

Proposition 3.1. *Assuming that the price function P is Lipschitz continuous, then there exists a unique solution to the system (6a)–(6b).*

To prove the previous result, we first study the forward system analogous to (6). More precisely, we consider the following system of ODEs,

$$\dot{X}_t = -\delta X_t + \frac{1}{\beta}(u_t - \alpha)^+, \quad \dot{u}_t = (r+\delta)u_t - (P(X_t) - c)\, h, \quad t \in [0,T], \tag{7}$$

with initial condition $(X_0, u_0) \in \mathbb{R}_+ \times \mathbb{R}$.

Lemma 3.1. *If P is Lipschitz continuous, then there exists a unique solution (X,u) to the initial value problem (7). Moreover, a comparison result holds, in the sense that if (X,u) and $(\tilde{X},\tilde{u})$ are solutions to (7), starting from (X_0,u_0) and $(X_0,\tilde{u}_0)$ respectively with $u_0 < \tilde{u}_0$, then $X_t \le \tilde{X}_t$ and $u_t < \tilde{u}_t$ for all $t \in [0,T]$.*

Proof of Lemma 3.1. Letting $\boldsymbol{x}_t := (X_t, u_t)$, we can rewrite the system (7) of two ODEs as $\dot{\boldsymbol{x}}_t = f(\boldsymbol{x}_t)$, starting from $\boldsymbol{x}_0 := (X_0, u_0)$. Since the price function P is assumed to be Lipschitz continuous, the generator f is also Lipschitz, so existence and uniqueness holds on $[0,T]$ by the Picard–Lindelöf theorem for this initial value problem. Note that, in particular, the solution satisfies for $t \in [0,T]$,

$$X_t = X_0 \mathrm{e}^{-\delta t} + \frac{1}{\beta}\int_0^t \mathrm{e}^{-\delta(t-s)}(u_s - \alpha)^+ \mathrm{d}s, \tag{8a}$$

$$u_t = u_0 \mathrm{e}^{(r+\delta)t} - h\int_0^t \mathrm{e}^{(r+\delta)(t-s)}(P(X_s) - c)\mathrm{d}s. \tag{8b}$$

Let then (X, u) and $(\tilde{X}, \tilde{u})$ be solutions to (7), starting from (X_0, u_0) and $(X_0, \tilde{u}_0)$ respectively, with $u_0 < \tilde{u}_0$. To establish the comparison result, we proceed by contradiction: let $t \in [0, T]$ be the smallest time for which $u_t = \tilde{u}_t$, meaning that $u_s \leq \tilde{u}_s$ for $s \in [0, t]$. From (8a), we have $X_s \leq \tilde{X}_s$, and using further that P is decreasing, we deduce $P(X_s) \geq P(\tilde{X}_s)$, for all $s \in [0, t]$. Using this in (8b), we obtain

$$\begin{aligned} u_t &\leq u_0 \mathrm{e}^{(r+\delta)t} - h \int_0^t \mathrm{e}^{(r+\delta)(t-s)} (P(\tilde{X}_s) - c) \mathrm{d}s \\ &< \tilde{u}_0 \mathrm{e}^{(r+\delta)s} - h \int_0^t \mathrm{e}^{(r+\delta)(t-s)} (P(\tilde{X}_s) - c) \mathrm{d}s = \tilde{u}_t, \end{aligned}$$

which leads to a contradiction, since we assumed $u_t = \tilde{u}_t$. In other words, for all $t \in [0, T]$ we have $u_t < \tilde{u}_t$, implying by (8a) that $X_t \leq \tilde{X}_t$. □

By the previous lemma, it suffices to show existence and uniqueness of $u_0 \in \mathbb{R}$ such that the solution (X, u) to (7) starting from (X_0, u_0) satisfies $u_T = 0$ to prove Proposition 3.1.

Proof of Proposition 3.1. Let (X, u) and $(\tilde{X}, \tilde{u})$ be solutions to (7), starting from (X_0, u_0) and $(X_0, \tilde{u}_0)$ respectively, and assume without loss of generality that $u_0 > \tilde{u}_0$. Define then $\Delta(t) \coloneqq u_t - \tilde{u}_t$ which is positive by Lemma 3.1 for all $t \in [0, T]$. Recall that we also have $X_t \geq \tilde{X}_t$, implying $P(X_t) \leq P(\tilde{X}_t)$, $t \in [0, T]$. Starting from (8b), and using in addition that P is L-Lipschitz continuous for $L \geq 0$, we obtain,

$$\begin{aligned} \Delta(T) &= (u_0 - \tilde{u}_0) \mathrm{e}^{(r+\delta)T} + h \int_0^T \mathrm{e}^{(r+\delta)(T-t)} (P(\tilde{X}_t) - P(X_t)) \mathrm{d}t \\ &\leq \Delta(0) \mathrm{e}^{(r+\delta)T} + hL \int_0^T \mathrm{e}^{(r+\delta)(T-t)} (X_t - \tilde{X}_t) \mathrm{d}t. \end{aligned}$$

Using now (8a), we have

$$X_t - \tilde{X}_t = \frac{1}{\beta} \int_0^t \mathrm{e}^{-\delta(t-s)} ((u_s - \alpha)^+ - (\tilde{u}_s - \alpha)^+) \mathrm{d}s,$$

and substituting into the previous inequality, we deduce

$$\begin{aligned} \Delta(T) &\leq \Delta(0) \mathrm{e}^{(r+\delta)T} + \frac{hL}{\beta} \int_0^T \int_0^t \mathrm{e}^{(r+\delta)(T-t)} \mathrm{e}^{-\delta(t-s)} ((u_s - \alpha)^+ - (\tilde{u}_s - \alpha)^+) \mathrm{d}s \mathrm{d}t \\ &\leq \Delta(0) \mathrm{e}^{(r+\delta)T} + \frac{hL}{\beta} \int_0^T \int_0^t \mathrm{e}^{(r+\delta)(T-t)} \mathrm{e}^{-\delta(t-s)} (u_s - \tilde{u}_s) \mathrm{d}s \, \mathrm{d}t \\ &\leq \Delta(0) \mathrm{e}^{(r+\delta)T} + \frac{hLM}{\beta} \int_0^T \Delta(t) \, \mathrm{d}t, \end{aligned}$$

where M is a constant depending on δ, r and T. Then, by Gronwall's Lemma, we deduce

$$\Delta(T) \coloneqq u_T - \tilde{u}_T \leq (u_0 - \tilde{u}_0) \mathrm{e}^{\left(r+\delta+\frac{hLM}{2\beta}\right)T}.$$

As the case $u_0 < \tilde{u}_0$ can be treated similarly, we conclude that the map $u_0 \in \mathbb{R} \longmapsto u_T \in \mathbb{R}$ is Lipchitz continuous.

In addition, we can show that this continuous map is negative for u_0 sufficiently small, and positive for u_0 sufficiently large. Indeed, on the one hand, if

$$u_0 < h \min_{t\in[0,T]} \int_0^t \mathrm{e}^{-(r+\delta)s}(P(X_0\mathrm{e}^{-\delta s}) - c)\mathrm{d}s,$$

which is non-positive, so in particular smaller than α, then the forward system (7) admits the following solution

$$X_t = X_0\mathrm{e}^{-\delta t}, \quad u_t = u_0\mathrm{e}^{(r+\delta)t} - h\int_0^t \mathrm{e}^{-(r+\delta)(s-t)}(P(X_s) - c)\mathrm{d}s, \quad t \in [0,T].$$

By the condition on u_0 above, we have $u_t < 0$ for all $t \in [0,T]$, so in particular $u_T < 0$ as wanted. On the other hand, recall that $X_t \geq X_0\mathrm{e}^{-\delta t}$ for all $t \in [0,T]$ by (3), implying since P is decreasing that $P(X_t) \leq P(X_0\mathrm{e}^{-\delta t})$, which is a positive constant. We then have

$$u_T \geq u_0\mathrm{e}^{(r+\delta)T} - h\int_0^T (P(X_0\mathrm{e}^{-\delta t}) - c)\mathrm{e}^{(r+\delta)(T-t)}\mathrm{d}t,$$

and thus taking

$$u_0 > h\int_0^T (P(X_0\mathrm{e}^{-\delta t}) - c)\mathrm{e}^{-(r+\delta)t}\mathrm{d}t,$$

we obtain $u_T > 0$.

From the previous reasoning, we deduce that the continuous map $u_0 \in \mathbb{R} \longmapsto u_T \in \mathbb{R}$ has values of opposite sign on $\mathbb{R}$, and thus has a root by Bolzano's theorem. In other words, there exists $u_0 \in \mathbb{R}$ such that $u_T = 0$, which concludes the existence part. Uniqueness follows directly from Lemma 3.1. Indeed, by the comparison principle, one necessarily needs $u_0 = \tilde{u}_0$ to ensure $u_T = \tilde{u}_T = 0$. □

To ensure existence and uniqueness of the solution to the forward-backward system (6a)–(6b), we now work under the assumption that the strictly decreasing price function P is Lipschitz continuous. In addition to this main result, we can establish some properties of the total installed capacity over time. We begin by constructing a trivial solution under a specific condition on the model parameters.

Lemma 3.2. *If the parameters $(r, \delta, T, h, \alpha, c, X_0)$ and the price function P are such that*

$$h\int_t^T \mathrm{e}^{-(r+\delta)(s-t)}(P(X_0\mathrm{e}^{-\delta s}) - c)\,\mathrm{d}s \leq \alpha, \quad \text{for all } t \in [0,T],$$

then the unique solution to the system (6a)–(6b) is given by

$$(X_t, u_t) = \left(X_0\mathrm{e}^{-\delta t}, h\int_t^T \mathrm{e}^{-(r+\delta)(s-t)}(P(X_0\mathrm{e}^{-\delta s}) - c)\,\mathrm{d}s\right), \quad t \in [0,T], \tag{9}$$

with corresponding optimal installation rate $K \equiv 0$.

Proof. Consider the candidate solution (9) provided in the lemma. By assumption, one has $u_t \leq \alpha$ for all $t \in [0,T]$, implying that

$$K_t = \frac{1}{\beta}(u_t - \alpha)^+ = 0, \quad t \in [0,T].$$

It is then straightforward to verify that the candidate solution (9) satisfies (6a)–(6b). □

The previous result highlights that if T or h are sufficiently small, or conversely if r, c, α or X_0 are sufficiently large, then there will be no new capacity installed at any time. As such model will be less interesting to study, we are led to make the following assumption, which will be verified in the numerical experimentation in Section 3.3, in particular for the parameters chosen in (13).

Assumption 3.1. *The model parameters $(r, \delta, T, h, \alpha, c, X_0)$ and the price function P are such that $(P(X_0) - c)h > (r+\delta)\alpha$ and there exists a time $t_0 \in [0,T]$ for which*

$$h \int_{t_0}^{T} \mathrm{e}^{-(r+\delta)(s-t_0)}(P(X_0\mathrm{e}^{-\delta s}) - c)\mathrm{d}s > \alpha.$$

Under the previous assumption, the unique solution (X,u) to the system (6a)–(6b) is not trivial, and exhibits some interesting properties, as stated in the following lemmas.

Lemma 3.3. *Under Assumption 3.1, there exists $T^\star \in (0,T)$ such that $u_t \geq \alpha$ for $t \leq T^\star$ and $u_t \leq \alpha$ for $t \geq T^\star$.*

Proof. First, if $u_t \leq \alpha$ for all $t \in [0,T]$, then the corresponding optimal installation rate is $K \equiv 0$, leading to the solution derived in (9). In particular, we have

$$u_t = h \int_t^T \mathrm{e}^{-(r+\delta)(s-t)}(P(X_0\mathrm{e}^{-\delta s}) - c)\,\mathrm{d}s \leq \alpha, \quad t \in [0,T],$$

which contradicts Assumption 3.1. Thus, there exists at least one $t \in [0,T]$ such that $u_t > \alpha$.

We then prove by contradiction that $u_0 > \alpha$. In particular, we assume that $u_0 \leq \alpha$ and take the first $t \in [0,T]$ for which $u_t = \alpha$, which exists by the above reasoning. In this case, we have $\dot{u}_t \geq 0$, and $u_s \leq \alpha$ for $s \in [0,t]$. This gives $K_s = 0$ for all $s \in [0,t]$, implying $X_t = X_0\mathrm{e}^{-\delta t} > X_0$. Using in addition that the price function P is strictly decreasing, we derive from (6b) the following inequality

$$0 \leq \dot{u}_t = (r+\delta)u_t - (P(X_t) - c)\,h \leq (r+\delta)\alpha - (P(X_0) - c)\,.$$

However, by Assumption 3.1, the right hand side is negative, leading to a contradiction.

To summarize, we necessarily have $u_0 > \alpha$ and $u_T = 0$. Then by continuity, there exists a time $T^\star \in [0,T]$ such that $u_{T^\star} = \alpha$. It remains to show that $u_t \geq \alpha$ on $t \in [0,T^\star]$ and $u_t \leq \alpha$ on $t \in [T^\star,T]$. We also proceed by contradiction, assuming that there exists an interval $[t_1,t_2] \subset [0,T]$ such that $u_{t_1} = u_{t_2} = \alpha$ and $u_s < \alpha$ for $s \in (t_1,t_2)$. On this interval,

the installation rate is zero and the capacity decays at rate δ. Mathematically, $X_{t_1} > X_{t_2}$, and thus $P(X_{t_1}) \leq P(X_{t_2})$. Using again (6b), we obtain

$$\dot{u}_{t_1} = (r+\delta)u_{t_1} - (P(X_{t_1}) - c)h \geq (r+\delta)u_{t_2} - (P(X_{t_2}) - c)h = \dot{u}_{t_2},$$

and since $\dot{u}_{t_1} \leq 0 \leq \dot{u}_{t_2}$, we necessarily have $\dot{u}_{t_1} = \dot{u}_{t_2} = 0$, which contradicts the fact that $u_s < \alpha$ for $s \in (t_1, t_2)$. Therefore, such interval cannot exist. In other words, if u drops strictly below α at some point, it cannot cross back to α afterwards. Since $u_0 > \alpha$ and $u_T = 0$, this concludes the proof of existence of $T^\star$ as required in the lemma. □

We can now prove that the price will stay above the production cost.

Lemma 3.4. *Under Assumption 3.1, we have $P(X_t) \geq c$ for all $t \in [0, T]$.*

Proof. Let $T^\star \in [0, T]$ given by Lemma 3.3. We first prove that $P(X_t) \geq c$ for all $t \in [T^\star, T]$. At time $T^\star$, we have by definition $u_{T^\star} = \alpha$ and $\dot{u}_{T^\star} \leq 0$, implying using (6b) that

$$0 \geq \dot{u}_{T^\star} = (r+\delta)u_{T^\star} - (P(X_{T^\star}) - c)h = (r+\delta)\alpha - (P(X_{T^\star}) - c)h.$$

In particular, $P(X_{T^\star}) - c \geq 0$. Moreover, for $t \geq T^\star$, we have $u_t \leq \alpha$, and therefore X satisfies the ODE $\dot{X}_t + \delta X_t = 0$. In other words, X decay at rate δ starting from $T^\star$, and thus $P(X_t) \geq P(X_{T^\star}) \geq c$ for $t \geq T^\star$.

We now prove the inequality for $t \in [0, T^\star]$, assuming by contradiction that $P(X_s) < c$ for some $s \in [0, T^\star]$. Note that by Assumption 3.1 and the previous reasoning, we have

$$P(X_0) > \frac{r+\delta}{h}\alpha + c \geq c, \quad \text{and} \quad P(X_{T^\star}) \geq c.$$

Therefore, there must exist an interval $(t_1, t_2) \subset [0, T^\star]$ for $t_1 < t_2 < T^\star$, on which $P(X_t) < c$ and $P(X_{t_1}) = P(X_{t_2}) = c$, with P being decreasing near t_1 and increasing near t_2. More precisely, there exists $\varepsilon > 0$ such that $P(X_t) \geq c$ for $t \in [t_1 - \varepsilon, t_1] \cup [t_2, t_2 + \epsilon]$, while $P(X_t) < c$ for $t \in (t_1, t_2)$. Since P is strictly decreasing, we have $X_{t_1} = X_{t_2} = P^{-1}(c)$, where P^{-1} denotes the inverse of P, and $\dot{X}_{t_1} \geq \dot{X}_{t_2}$. Moreover, since $t_1 < t_2 < T^\star$, we have by Lemma 3.3 that $u_t \geq \alpha$ for $t \in [t_1, t_2]$. The system of equations satisfied by the solution (X, u) on the interval (t_1, t_2) is thus

$$\dot{X}_t + \delta X_t = \frac{1}{\beta}(u_t - \alpha), \qquad \dot{u}_t = (r+\delta)u_t - h(P(X_t) - c).$$

Since $P(X_t) < c$ for $t \in (t_1, t_2)$, we have $\dot{u}_t > 0$, and thus $u_{t_1} < u_{t_2}$. However, this is in contradiction with the fact that $X_{t_1} = X_{t_2} = P^{-1}(c)$ and $\dot{X}_{t_1} \geq 0 \geq \dot{X}_{t_2}$, since

$$\frac{1}{\beta}(u_{t_1} - \alpha) = \dot{X}_{t_1} + \delta X_{t_1} = \dot{X}_{t_1} + \delta P^{-1}(c) \geq \dot{X}_{t_2} + \delta P^{-1}(c) = \dot{X}_{t_2} + \delta X_{t_2} = \frac{1}{\beta}(u_{t_2} - \alpha).$$

This concludes the proof that $P(X_t) \geq c$ for all $t \in [0, T]$. □

Under Assumption 3.1, and thanks to Lemma 3.3, we have $u_t \geq \alpha$ for $t \leq T^\star$ and $u_t \leq \alpha$ for $t \geq T^\star$. In particular, on $t \leq T^\star$, the ODE (6a) for X becomes

$$\dot{X}_t + \delta X_t = \frac{1}{\beta}(u_t - \alpha).$$

Differentiating the previous ODE and replacing $\dot{u}$ using (6b) yields the following two-point boundary value problem,

$$\ddot{X}_t = r\dot{X}_t + (r+\delta)\left(\delta X_t + \frac{\alpha}{\beta}\right) - \frac{h}{\beta}\left(P(X_t) - c\right), \tag{10}$$

with boundary conditions $X_0 \geq 0$ fixed and $\delta X_{T^\star} + \dot{X}_{T^\star} = 0$, since $u_{T^\star} = \alpha$. Then, for $t \geq T^\star$, we have $u_t \leq \alpha$, implying in particular that there is no installation after time $T^\star$. We deduce that for $t \in [T^\star, T]$,

$$X_t = X_{T^\star}\mathrm{e}^{-\delta(t-T^\star)}, \quad u_{T^\star} = h\int_{T^\star}^{T} \mathrm{e}^{-(r+\delta)(t-T^\star)}(P(X_{T^\star}\mathrm{e}^{-\delta(t-T^\star)}) - c)\mathrm{d}t = \alpha.$$

3.2 Linear price function

In this section, we focus on the price P being a linear decreasing function, *i.e.*

$$P(x) = d_1 - d_2 x \quad \text{for some } d_1, d_2 > 0,$$

and assume Assumption 3.1 is satisfied. Under this linear specification for the price, we can obtain a semi-explicit formula for the optimal capacity.

Proposition 3.2. *For a linear price function as above, we have*

$$X_t = \begin{cases} C\mathrm{e}^{r_1 t} + D\mathrm{e}^{r_2 t} + \theta, & \text{for } t \leq T^\star, \\ X_{T^\star}\mathrm{e}^{-\delta(t-T^\star)}, & \text{for } t \in [T^\star, T], \end{cases} \tag{11}$$

$$\text{with} \quad \theta := \frac{h(d_1 - c) - (r+\delta)\alpha}{\beta(r+\delta)\delta + hd_2}, \; C := \frac{(X_0+\theta)(r_2+\delta) - \delta\theta\mathrm{e}^{-r_2 T^\star}}{(r_2+\delta) - \mathrm{e}^{(r_1-r_2)T^\star}(r_1+\delta)}, \; D := X_0 - C - \theta,$$

$$\text{and} \quad r_{1,2} := \frac{1}{2}\left(r \pm \sqrt{r^2 + 4\left((r+\delta)\delta + \frac{h}{\beta}d_2\right)}\right),$$

and where $T^\star$ is solution to the following transcendental equation,

$$\alpha = \frac{h(d_1-c)}{r+\delta}(1 - \mathrm{e}^{-(r+\delta)(T-T^\star)}) - \frac{hd_2}{r+2\delta}(1 - \mathrm{e}^{-(r+2\delta)(T-T^\star)})(C\mathrm{e}^{r_1 T^\star} + D\mathrm{e}^{r_2 T^\star} + \theta). \tag{12}$$

Proof. Recall that $T^\star$ is defined in Lemma 3.3. As already mentioned, there is no installation after time $T^\star$, thus $X_t = X_{T^\star}\mathrm{e}^{-\delta(t-T^\star)}$ for $t \in [T^\star, T]$ as stated in (11). For $t \leq T^\star$, using the linear price in (10) we derive

$$\ddot{X}_t - r\dot{X}_t - \left((r+\delta)\delta + \frac{h}{\beta}d_2\right)X_t = \frac{1}{\beta}\left(\alpha(r+\delta) - h(d_1 - c)\right),$$

with boundary conditions $X_0 \geq 0$ fixed and $\delta X_{T^\star} + \dot{X}_{T^\star} = 0$. Straightforward, albeit lengthy, computations show that the candidate solution X defined in (11) is indeed solution to this second-order linear ODE boundary-value problem. In particular, r_1, r_2 are the two solutions of the quadratic equation $x^2 - rx - \left((r+\delta)\delta + \frac{h}{\beta} d_2\right) = 0$, with $r_1 > r + \delta > -\delta > r_2$. The constants C and D are derived from the boundary conditions. We further verify that the denominator in the definition of C is not zero, because $r_2 + \delta < 0 < r_1 + \delta$. Finally, we find $T^\star \in (0, T)$ from $u_{T^\star} = \alpha$, which leads to (12). Finding $T^\star$ from this equation fully determines C, and thus D, which describe the solution X. □

Since the linear price is Lipschitz continuous, the previous solution is unique by Proposition 3.1, implying in particular that there exists a unique solution $T^\star$ to Equation (12). This will also be observed numerically in the following section.

3.3 Numerical solution

In this section, we numerically solve (6a)–(6b) for two different price functions P, linear—as in the previous section—and inverse, and for the parameters used in [2, 5]:

$$\begin{aligned} X_0 = 30\text{GW}, \quad c = 15\$/\text{MWh}, \quad r = 0.1\text{year}^{-1}, \quad \delta = \frac{\log 2}{10}\text{year}^{-1}, \\ h = 3000\frac{\text{hours}}{\text{year}}, \quad \alpha = 1400\$/\text{kW}, \quad \frac{1}{\beta} = 5\text{MW}^2/(\$\text{year}). \end{aligned} \tag{13}$$

The comparison principle in Lemma 3.1 suggests a shooting method to numerically solve the forward-backward system (6a)–(6b): starting from an arbitrary value u_0, one can solve the forward system (7) to obtain u_T, and then update the choice of u_0 depending on the sign of u_T. More precisely, by the comparison principle, one should increase the guess for u_0 if $u_T < 0$, and decrease otherwise. Since both the linear and inverse price functions are assumed to be Lipschitz continuous, this shooting method is guaranteed to converge to the unique solution.

Linear price function. The previous numerical scheme is first implemented for a linear price function of the form $P(x) = d_1 - d_2 x$ with $d_1 = 500\$/\text{MWh}$, $d_2 = 10^{-2}\$/\text{MW}^2\text{h}$, and compared with another numerical method, consisting of computing $T^\star$ by numerically solving (12) and then replacing in the explicit formulas established in Proposition 3.2. The results are displayed in Figure 1 for a fixed time horizon $T = 5$. More precisely, Figure 1a illustrates how to find $T^\star$ such that (12) is satisfied. Then, Figure 1b confirms that the solution obtained with the shooting method coincides on $[0, T]$ with the semi-explicit solution.

The main economic observation from the numerical results illustrated in Figure 1b is the decay of capacity at the natural rate δ after the critical time $T^\star \approx 0.25$. More precisely, the total installed capacity initially increases rapidly, reflecting the strong early incentives to invest. However, due to the finite planning horizon, a critical threshold time $T^\star$ emerges, beyond which further investment is no longer profitable. This behavior contrasts sharply with the infinite-horizon results of [5], where investment incentives remain constant over time. Indeed, in our finite time horizon setting, since no profits can be generated after

time T, producers find it optimal to cease installing new capacity sufficiently in advance of the terminal date to avoid incurring costs that cannot be recouped. In other words, once the remaining time falls below a certain threshold, the opportunity cost of investment outweighs any remaining benefits. Consequently, investment stops, and capacity decays passively at the rate δ, in line with the theoretical predictions established in Lemma 3.3. This numerical example thus provides a clear illustration of how finite-horizon considerations fundamentally alter investment dynamics compared to the infinite-horizon benchmark.

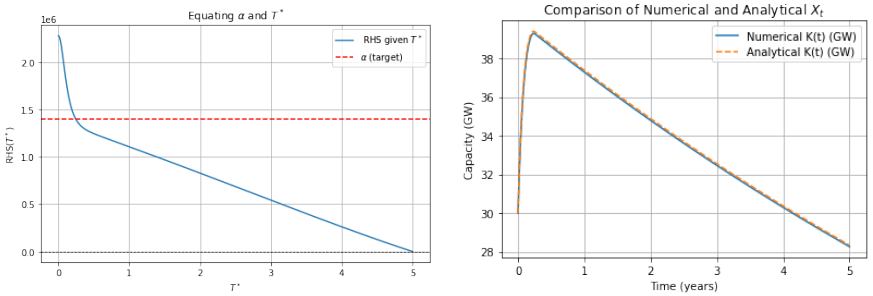

(a) α and $T^\star$ equation (b) Capacity dynamics

Figure 1: Capacity dynamics and corresponding $T^\star$ with linear price function

Inverse price function. We then consider as in [5] an 'inverse' price function of the form $P(x) = p/x$, for $p = 6.5 \times 10^6$\$/h and the parameters previously described in (13). We first emphasize that, although the price function $P(x) = p/x$ is not Lipschitz continuous on $\mathbb{R}_+$, this does not cause issues for the dynamics. Indeed, the installed capacity X_t satisfies the lower bound $X_t \geq X_0 e^{-\delta t}$, where $X_0 > 0$ is the initial capacity. Thus, X_t remains bounded away from 0 for all $t \in [0, T]$, and $P(x)$ is effectively Lipschitz on the reachable set $\{x \geq X_0 e^{-\delta T}\}$. This guarantees the well-posedness of the solution.

Figure 2 presents the dynamics of the total capacity X over time in the case of an inverse price function, for three different finite time horizons ($T = 5$, 10, and 20 years). We first observe that the solution satisfies Lemma 3.3: as in the previous case with a linear price, there is an initial increase in total capacity, followed by decay at the natural rate δ.

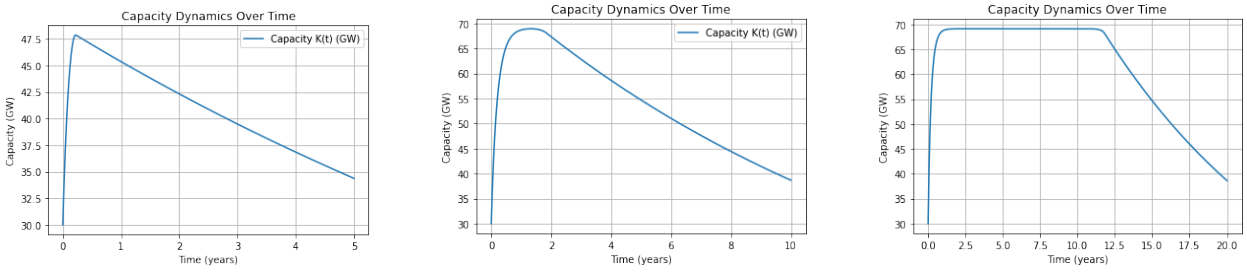

(a) $T = 5$ years (b) $T = 10$ years (c) $T = 20$ years

Figure 2: Capacity dynamics with inverse price function for different time horizons

For the longest time horizons ($T = 20$ years), the total capacity rapidly approaches

the infinite-horizon stationary state studied in [5], and remains near this steady state for most of the planning horizon. This illustrates a form of *turnpike effect* (see, for *e.g.* [12]): for sufficiently large maturity, the optimal policy drives the system close to the long-run equilibrium early on and maintains it there as long as 'possible', *i.e.* here until it is no longer profitable to invest. Interestingly, when the horizon is larger than 10 years, the simulations indicate that the cessation of investment occurs approximately 8.5 years before the terminal date, suggesting that the critical time $T^\star \approx T - 8.5$ for the given parameters.

In contrast, when the planning horizon is short (*e.g.*, $T = 5$), the total capacity increases briefly but remains below the infinite-horizon steady state, before decaying at the natural rate δ, as also seen in Figure 1b for the linear price case with the same maturity. This behavior reflects the fact that producers anticipate the approaching horizon and adjust their decisions to avoid incurring installation costs that cannot be recovered.

4 Heterogeneous producers

We now approximate the finite player game by one in which there is a continuum of producers whose capacities at time $t = 0$ are distributed according to the continuous density function $m_0(x)$ on $x \geq 0$, which smooths out the actual discrete (empirical) distributions of initial installed capacities $(x_0^{(i)})_{i\in\{0,\dots,N\}}$.

In the approximating MFG, we consider x_t the installed capacity of a representative producer at time $t \in [0, T]$. Analogous to (1), we have

$$\mathrm{d}x_t = (-\delta x_t + \nu_t)\,\mathrm{d}t, \tag{14}$$

where ν_t is their installation rate at time $t \in [0, T]$. We then let $\bar{x}_t$ and $\bar{\nu}_t$ denote, respectively, the mean installed capacity and mean installation rate at time t. We adopt the following approximations of the aggregate quantities X and K,

$$X_t \coloneqq \sum_{j=0}^{N} x_t^{(j)} \approx x_t + N\bar{x}_t, \qquad K_t \coloneqq \sum_{j=0}^{N} \nu_t^{(j)} \approx \nu_t + N\bar{\nu}_t, \quad t \in [0, T], \tag{15}$$

which restore the individual impacts on the aggregates, in the sense that now

$$\frac{\partial X_t}{\partial x_t} = 1, \quad \text{and} \quad \frac{\partial K_t}{\partial \nu_t} = 1.$$

This continuum aggregate game approximation was used in the cryptocurrency-mining model in [26], and is further analyzed in [22]. This can also be related to what is called λ-*interpolated mean field games*, introduced in [14] and generalized in [17]. As we will see in Lemma 4.1, under the preceding approximations and the additional concavity assumption on the function $x \longmapsto xP(x + N\bar{x})$, producers with smaller installed capacity achieve a higher profit per unit of new energy installed than producers with larger capacity. This, in turn, results in a higher installation rate for smaller producers.

Using the approximations (15) in the original objective (5), we are led to consider the following dynamic value function, for $(t,x) \in [0,T] \times \mathbb{R}_+$,

$$V(t,x) = \sup_{\nu \geq 0} \int_t^T \mathrm{e}^{-r(s-t)} \Big[(P(x_s + N\bar{x}_s) - c) h x_s - \nu_s(\alpha + \beta(\nu_s + N\bar{\nu}_s)) \Big] \, \mathrm{d}s. \tag{16}$$

For fixed continuum mean quantities $\bar{x}$ and $\bar{\nu}$, the representative producer's Hamiltonian is

$$\sup_{\nu_t \geq 0} \left\{ \left(P(x + N\bar{x}_t) - c\right) hx - \nu_t(\alpha + \beta(\nu_t + N\bar{\nu}_t)) + \frac{\partial V}{\partial x} \left(-\delta x + \nu_t\right) \right\},$$

from which we derive the associated optimal response

$$\nu^\star(t,x) = \frac{1}{2\beta} \left(\frac{\partial V}{\partial x} - \alpha - \beta N \bar{\nu}_t \right)^+, \quad (t,x) \in [0,T] \times \mathbb{R}_+. \tag{17}$$

The value function defined in (16) then satisfies the following Hamilton-Jacobi-Bellman (HJB) equation:

$$\frac{\partial V}{\partial t} - rV - \delta x \frac{\partial V}{\partial x} + (P(x + N\bar{x}_t) - c)hx + \frac{1}{4\beta} \left[\left(\frac{\partial V}{\partial x} - \alpha - \beta N \bar{\nu}_t \right)^+ \right]^2 = 0, \tag{18}$$

for $(t,x) \in [0,T) \times \mathbb{R}_+$, with terminal condition $V(T,x) = 0$. The associated Fokker-Planck (FP) equation for the density $m(t,x)$ of installed capacities at time $t > 0$ is

$$\frac{\partial}{\partial t} m + \frac{\partial}{\partial x} \left[m \left(-\delta x + \frac{1}{2\beta} \left(\frac{\partial V}{\partial x} - \alpha - \beta N \bar{\nu}_t \right)^+ \right) \right] = 0, \tag{19}$$

with given initial condition $m(0,x) = m_0(x)$. The preceding system of equations (18)–(19) characterizes a mean field game of state and control, approximating the original N-player game. Integrating (17) over $m(t,\cdot)$ and rearranging yields to the following fixed-point condition for the mean installation rate at equilibrium,

$$\bar{\nu}_t = \frac{\int_{\mathcal{A}_t} (\frac{\partial V}{\partial x} - \alpha) m(t,x) \mathrm{d}x}{2\beta + \beta N \int_{\mathcal{A}_t} m(t,x) \, \mathrm{d}x}, \quad \text{with } \mathcal{A}_t \coloneqq \left\{ x : \frac{\partial V}{\partial x} - \alpha - \beta N \bar{\nu}_t > 0 \right\}, \quad t \in [0,T]. \tag{20}$$

The dynamics of the mean state at the mean field equilibrium is then given by

$$\dot{\bar{x}}_t + \delta \bar{x}_t = \bar{\nu}_t, \quad t \in [0,T],$$

with initial condition $\bar{x}_0 = \int x m_0(x) \, \mathrm{d}x$.

In Section 4.1 we will explain how this mean field approximation generalize the case of homogeneous producers studied in Section 3. Then, in Section 4.2, we will prove some preliminary results on the value function that will be helpful to solve in Section 4.3 the HJB–FP system (18)–(19).

4.1 Connection to the homogeneous producers case

Under the following simplifications, one recovers the specific setting studied in Section 3:

(i) All producers start with the same capacity.

(ii) There is no direct individual impact on the price.

First, by (i), the producers remain indistinguishable at all times, in the sense that their individual capacities are all identical, and in particular $m(t,\cdot)$ is a Dirac delta function for every $t \in [0,T]$. Moreover, their optimal controls coincide, and we thus deduce from (17)

$$\bar{\nu}_t = \nu^\star(t,x_t) = \frac{1}{\beta(N+2)}\left(\frac{\partial V}{\partial x}(t,x_t) - \alpha\right)^+, \quad t \in [0,T],$$

which coincide with (20) because either the measure of m is positive in $\mathcal{A}_t$ or it is zero and $\frac{\partial V}{\partial x} \le \alpha$ on $\mathcal{A}_t$. Using this in the dynamic of the mean state $\bar{x}$ at the mean field equilibrium, with the approximation $\frac{N+1}{N+2} \approx 1$, we derive the required dynamics for the total capacity $X_t = (N+1)\bar{x}_t$, namely

$$\dot{X}_t + \delta X_t = \frac{1}{\beta}(u_t - \alpha)^+, \quad \text{with } u_t := \frac{\partial V}{\partial x}(t,x_t), \quad t \in [0,T]. \tag{21}$$

It remains to compute the dynamics of u_t defined above, the marginal value along the optimal trajectory, in the spirit of Hotelling's rule for the economics of exhaustible resources (see [15] for a MFG version). First, by (ii), an individual producer has no direct impact on the price, meaning that its impact is only through the mean capacity. This boils down to replacing $P(x_t + N\bar{x}_t)$ by $P((N+1)\bar{x}_t)$, or $P(X_t)$ for fixed total capacity X_t, $t \in [0,T]$. Using this in (18), and differentiating with respect to the individual capacity x, we obtain

$$\frac{\partial^2 V}{\partial t \partial x} - r\frac{\partial V}{\partial x} - \delta\frac{\partial V}{\partial x} - \delta x_t \frac{\partial^2 V}{\partial x^2} + (P(X_t) - c)h + \frac{\left(\frac{\partial V}{\partial x} - \alpha - \beta N \bar{\nu}_t\right)^+}{2\beta}\frac{\partial^2 V}{\partial x^2} = 0.$$

Noticing that $\frac{1}{2\beta}\left(\frac{\partial V}{\partial x} - \alpha - \beta N\bar{\nu}_t\right)^+ = \nu^\star(t,x)$ and $-\delta x_t + \nu^\star(t,x_t) = \dot{x}_t$, the above PDE becomes

$$\frac{\partial^2 V}{\partial t \partial x} - (r+\delta)\frac{\partial V}{\partial x} + h(P(X_t) - c) + \dot{x}_t \frac{\partial^2 V}{\partial x^2} = 0.$$

Finally, by definition of u in (21) and using the chain rule $\dot{u}_t = \frac{\partial^2 V}{\partial t \partial x} + \dot{x}_t \frac{\partial^2 V}{\partial x^2}$, we deduce

$$\dot{u}_t = (r+\delta)u_t - h(P(X_t) - c), \tag{22}$$

with $u_T = 0$ since $V(T,x) = 0$. Therefore, under the two simplications (i)–(ii), the general HJB–FP system (18)–(19) boils down to the ODE system (22)–(21), which coincides with the system (6a)–(6b) studied in Section 3. The two methods, Pontryagin maximum principle and HJB, are thus consistent in this setting.

4.2 Properties of the value function

In this section, we establish several properties of the value function, which will guide the numerical resolution of (18)–(19). The following result highlights that producers with smaller capacity install at a larger rate. In fact, we will prove that the optimal strategy for producers with large capacity is to stop installing new capacity.

Lemma 4.1. *Assuming that the revenue $x \longmapsto xP(x+N\bar{x})$ is concave, then for all $t \in [0,T]$, $x \longmapsto V(t,x)$ is also concave, and $x \longmapsto \nu^\star(t,x)$ is non-increasing.*

Proof. Let $t \in [0,T]$, and consider two processes x and x' satisfying (14), respectively starting from x_t, x'_t at time t, and driven by two possibly different controls ν, ν'. In particular

$$x_s = x_t \mathrm{e}^{-\delta(s-t)} + \int_t^s \mathrm{e}^{-\delta(s-y)}\nu_y \mathrm{d}y, \quad \text{and} \quad x'_s = x'_t \mathrm{e}^{-\delta(s-t)} + \int_t^s \mathrm{e}^{-\delta(s-y)}\nu'_y \mathrm{d}y, \quad s \in [t,T].$$

Let $\lambda \in [0,1]$, define the process x^λ, starting from $x^\lambda_t := \lambda x_t + (1-\lambda)x'_t$ at time t, and driven by the admissible control $\nu^\lambda := \lambda\nu + (1-\lambda)\nu'$. Note that we have

$$x^\lambda_s = \lambda x_s + (1-\lambda)x'_s = x^\lambda_t \mathrm{e}^{-\delta(s-t)} + \int_t^s \mathrm{e}^{-\delta(s-y)}\nu^\lambda_y \mathrm{d}y, \quad s \in [t,T].$$

Let now $s \in [t,T]$. From the concavity assumption on $x \longmapsto (P(x+N\bar{x})-c)x$, we deduce

$$\lambda(P(x_s+N\bar{x}_s)-c)x_s + (1-\lambda)(P(x'_s+N\bar{x}_s)-c)x'_s \le (P(x^\lambda_s+N\bar{x}_s)-c)x^\lambda_s. \tag{23}$$

Moreover, since the cost is linear-quadratic, we also have

$$-\lambda\nu_s(\alpha+\beta\nu_s+\beta N\bar{\nu}_s) - (1-\lambda)\nu'_s(\alpha+\beta\nu'_s+\beta N\bar{\nu}_s) \le -\nu^\lambda_s(\alpha+\beta\nu^\lambda_s+\beta N\bar{\nu}_s). \tag{24}$$

Denoting by f the running reward in the definition of the value function V in (16), namely

$$f(x_s,\nu_s) := (hP(x_s+N\bar{x}_s)-c)x_s - \nu_s(\alpha+\beta(\nu_s+N\bar{\nu}_s)), \tag{25}$$

we obtain, by summing (23) and (24), the following inequality,

$$\lambda f(x_s,\nu_s) + (1-\lambda)f(x'_s,\nu'_s) \le f(x^\lambda_s,\nu^\lambda_s),$$

for all $s \in [t,T]$. Multiplying by $\mathrm{e}^{-r(s-t)}$ and integrating from t to T, we deduce

$$\lambda\int_t^T \mathrm{e}^{-r(s-t)}f(x_s,\nu_s)\mathrm{d}s + (1-\lambda)\int_t^T \mathrm{e}^{-r(s-t)}f(x'_s,\nu'_s)\mathrm{d}s \le \int_t^T \mathrm{e}^{-r(s-t)}f(x^\lambda_s,\nu^\lambda_s)\mathrm{d}s.$$

The RHS of the previous inequality is upper bounded by $V(t,x^\lambda_t) = V(t,\lambda x_t+(1-\lambda)x'_t)$. Finally, taking the supremum over the arbitrary controls ν and ν', we deduce

$$\lambda V(t,x_t) + (1-\lambda)V(t,x'_t) \le V(t,\lambda x_t+(1-\lambda)x'_t), \quad t \in [0,T].$$

Since x_t and x'_t are arbitrary, this completes the proof that the value function V is concave.

The fact that $\nu^\star(t,x)$ is decreasing in x is a direct consequence of the concavity of V. Indeed, since V is concave, $\frac{\partial V}{\partial x}$ is decreasing in x, implying that $\nu^\star(t,x) = \frac{1}{2\beta}(\frac{\partial V}{\partial x} - \alpha - \beta N\bar{\nu}_t)^+$ is non-increasing in x. □

In the following, we will work under the standing assumption stated in the previous lemma, namely that the mapping $x \longmapsto x\,P(x + N\bar{x})$ is concave. This assumption is satisfied in the examples of price functions we will consider, in particular the linear and inverse cases, discussed in Sections 4.3 and 4.4 respectively.

Lemma 4.2. *Suppose that* $\lim_{y\to\infty} P(y) < c$. *Then, there exists* $x_{\max} < \infty$ *such that, for all* $t \in [0,T]$ *and for any process* x *with dynamics defined by* (14) *and starting from* $x_t \geq x_{\max}\mathrm{e}^{-\delta t}$, *the associated optimal control is* $\nu^\star(s, x_s) = 0$ *for all* $s \in [t,T]$.

Proof. Since $\lim_{y\to\infty} P(y) < c$, there exists $q < \infty$ such that $P(q) < c$, and we can thus define $x_{\max} \coloneqq q\mathrm{e}^{\delta T}$. Let then $t \in [0,T]$. For any process x starting from $x_t \geq x_{\max}\mathrm{e}^{-\delta t}$ at time t, the non-negativity of both the capacities and the admissible control imply

$$x_s + N\bar{x}_s \geq x_s \geq x_t\mathrm{e}^{-\delta(s-t)} \geq x_{\max}\mathrm{e}^{-\delta s} \geq x_{\max}\mathrm{e}^{-\delta T} = q, \quad s \in [t,T],$$

and since P is decreasing with $P(q) < c$, we deduce that $P(x_s + N\bar{x}_s) - c < 0$ for all $s \in [t,T]$. Since the revenue at any time $s \in [t,T]$, namely $h(P(x_s + N\bar{x}_s) - c)x_s$, is negative, and the cost of installing new capacity is always non-negative, it is straightforward to conclude that no capacity should be installed on $[t,T]$. More precisely, let x as above, driven by a non trivial control ν, and starting from $x_t \geq x_{\max}\mathrm{e}^{-\delta t}$, and let x° the corresponding uncontrolled process, *i.e.* $x^\circ_s = x_t\mathrm{e}^{-\delta(s-t)}$, $s \in [t,T]$. We clearly have $x_s \geq x^\circ_s = x_t\mathrm{e}^{-\delta(s-t)} \geq q$, and by the previous remark on the negative revenue and non-negative cost, we deduce that

$$f(x^\circ_s, 0) > f(x_s, \nu_s), \qquad \text{for } \nu_s > 0, \quad s \in [t,T].$$

recalling that f is the running reward defined in (25). Multiplying by $\exp(-r(s-t))$ and integrating over $s \in [t,T]$, it follows that any nonzero control yields a strictly smaller total reward than applying no control. Consequently, the optimal control is $\nu \equiv 0$. □

By the previous lemma, we have that at any time t, $\nu^\star(t,x) = 0$ for x sufficiently large, namely $x \geq x_{\max}\mathrm{e}^{-\delta t}$. From Equation (17), we deduce that $\frac{\partial V}{\partial x} \leq \alpha + \beta N\bar{\nu}_t$ for $x \geq x_{\max}$. Since V is concave, the mapping $x \longmapsto \frac{\partial V}{\partial x}$ is decreasing. As a result, we define for $t \in [0,T]$ and fixed mean installation rate $\bar{\nu}_t$,

$$x^\star(t) = \begin{cases} \min\left\{x \geq 0 \;\middle|\; \frac{\partial V}{\partial x}(t,x) = \alpha + \beta N\bar{\nu}_t\right\}, & \text{if } \frac{\partial V}{\partial x}(t,0) \geq \alpha + \beta N\bar{\nu}_t \\ 0, & \text{if } \frac{\partial V}{\partial x}(t,0) < \alpha + \beta N\bar{\nu}_t. \end{cases}$$

The previous quantity $x^\star(t)$ defines a threshold capacity: producers with installed capacity $x < x^\star(t)$ at time t will invest to increase their capacity, whereas producers with capacity already exceeding this threshold will not invest. In addition, since $\nu^\star(T,x) = 0$, we deduce $x^\star(T) = 0$, and we can define $T^\star = \inf\{t \in [0,T] : x^\star(s) = 0,\ \forall s \in [t,T]\}$, which is the analogue of $T^\star$ in Lemma 3.3 for the homogeneous case. Note that at $T^\star$, since $x^\star(T^\star) = 0$, no producer should install new capacity, *i.e.* $\bar{\nu}_{T^\star} = 0$. Using this in the definition of $x^\star$ above, we deduce $\frac{\partial V}{\partial x}(T^\star, 0) = \alpha$. Since $\frac{\partial V}{\partial x}(T,0) = 0$, we conclude that $T^\star < T$. Note that after $T^\star$, $x^\star$ will stay at 0, meaning that no producer will install new capacity for the remaining time. This is illustrated in Figure 3 and confirmed by the numerical results in Section 4.3.

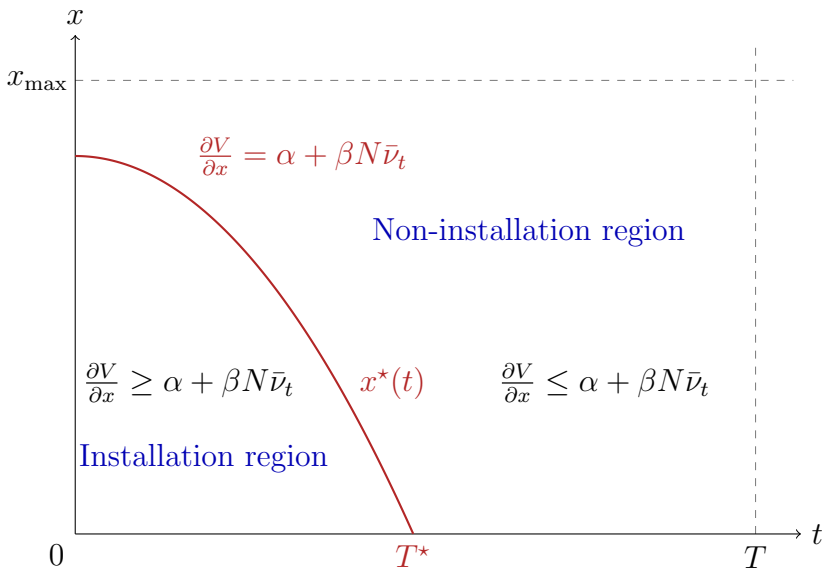

Figure 3: Installation and non-installation regions

In the following proposition, we provide a semi-explicit formula for the value function in the non-installation region, as illustrated in Figure 3. In particular, this result shows that if a producer does not install new capacity at some time $t \in [0, T]$, they will not invest at any later time $s \in [t, T]$. In other words, once a producer's capacity belongs to the non-installation region, it will remain in that region.

Proposition 4.1. *In the non-installation region* $\{(t, x) : x \geq x^\star(t)\}$, $V(t, x)$ *is given by*

$$V(t,x) = x \int_t^T \mathrm{e}^{-(r+\delta)(s-t)} h(P(N\bar{x}_s + x\mathrm{e}^{-\delta(s-t)}) - c)\,\mathrm{d}s. \tag{26}$$

Proof. First, in the non-installation region, the HJB equation (18) simplifies to

$$\frac{\partial V}{\partial t} - rV - \delta x \frac{\partial V}{\partial x} + h(P(x + N\bar{x}_t) - c)x = 0,$$

with terminal condition $V(T, x) = 0$, which is a linear PDE for which existence and uniqueness holds. It is then straightforward to see that the candidate solution in (26) indeed satisfies the above PDE. Clearly, V is also the value obtained under the trajectory $x_s = x_t \mathrm{e}^{-\delta(s-t)}$, which coincides with the strategy of no installation between t and T. □

4.3 Linear price function

In this section, we revisit the case of a linear price function $P(x) = d_1 - d_2 x$ with $d_1, d_2 > 0$, previously studied in Section 3.2 for the homogeneous case.

Corollary 4.1. *In the non-installation region* $\{(t,x) : x \geq x^\star(t)\}$*, the value function is given by* $V(t,x) = a_t x^2 + b_t x$ *with*

$$a_t = -\frac{hd_2}{r+2\delta}\left(1 - \mathrm{e}^{-(r+2\delta)(T-t)}\right), \quad b_t = h\int_t^T \mathrm{e}^{-(r+\delta)(s-t)}(d_1 - c - d_2 N \bar{x}_s)\,\mathrm{d}s \tag{27}$$

and the threshold curve is

$$x^\star(t) = \max\left(\frac{\alpha + \beta N \bar{\nu}_t - b_t}{2a_t}, 0\right), \quad \text{for } t < T. \tag{28}$$

Proof. Under the linear price specification, we can make the linear quadratic ansatz $V(t,x) = a_t x^2 + b_t x$. From Proposition 4.1, we directly deduce that the pair (a,b) is solution to the following system of ODE,

$$\dot{a}_t - r a_t - 2\delta a_t - h d_2 = 0, \quad \dot{b}_t - r b_t - \delta b_t + h(d_1 - c - d_2 \bar{x}_t N) = 0, \quad a_T = b_T = 0,$$

and thus given by (27). Finally, Equation (28) is derived from the fact that V satisfies $\frac{\partial V}{\partial x}(t, x^\star(t)) = \alpha + \beta N \bar{\nu}_t$ when $x^\star(t) > 0$. □

From the previous result, note that a_t is only a function of t, while b_t is expressed as a function of the trajectory of the mean installed capacity, namely $\bar{x}_s$ for $s \in [t,T]$. Unfortunately, such explicit derivation is not possible in the installation region. More precisely, on $\{(t,x) : x < x^\star(t)\}$, we have by definition that $\nu^\star > 0$, and the HJB equation (18) satisfied by the value function V becomes

$$\frac{\partial V}{\partial t} - rV - \delta x \frac{\partial V}{\partial x} + h(d_1 - c - d_2(x + \bar{x}_t N))x + \frac{1}{4\beta}\left(\frac{\partial V}{\partial x} - \alpha - \beta N \bar{\nu}_t\right)^2 = 0. \tag{29}$$

However, to our knowledge, no explicit solution exists for the previous HJB equation when the boundary condition is determined by the solution in the non-installation region, given by Corollary 4.1. Nevertheless, in the following, we suggest two numerical approaches to approximate the value function, the corresponding optimal strategy, and the solution to (19) in that region. The first approach uses a quadratic ansatz for approximation, while the second employs a finite difference scheme.

4.3.1 Linear-quadratic approximation

For the first numerical approach, we approximate the solution to PDE (29) by a quadratic function. More precisely, using the ansatz $V(t,x) = A_t x^2 + B_t x + C_t$ in (29), we obtain that the functions A, B, C should be solution to the system

$$\dot{A}_t = (r+2\delta)A_t + h d_2 - \frac{1}{\beta}A_t^2 \tag{30a}$$

$$\dot{B}_t = r B_t + \delta B_t - h(d_1 - c - d_2 \bar{x}_t N) - \frac{1}{\beta}A_t(B_t - \alpha - \beta N \bar{\nu}_t) \tag{30b}$$

$$\dot{C}_t = r C_t - \frac{1}{4\beta}((B_t - \alpha - \beta N \bar{\nu}_t)^+)^2. \tag{30c}$$

By (30a), A solves a Riccati equation, and therefore it will be of the form

$$A_t = \beta \frac{\lambda_1 + R_A \lambda_2 \mathrm{e}^{(\lambda_2 - \lambda_1)t}}{1 + R_A \mathrm{e}^{(\lambda_2 - \lambda_1)t}}$$

with $\lambda_1 > 0 > \lambda_2$ solutions to the quadratic equation $\lambda^2 - \beta(r + 2\delta)\lambda - h\beta d_2 = 0$ and R_A a constant to be determined. Similarly, from (30b), B depends on a constant R_B, which is the value of B at $T^\star$ and is similarly not known yet. We choose the above constants R_A and R_B so that $A_{T^\star} = 0$, since concavity of V requires $A \leq 0$, and $B_{T^\star} = b_{T^\star}$, to ensure that $\frac{\partial V}{\partial x}$ matches at the point $(T^\star, 0)$ with the solution in the non-installation region. Note that we do not impose the smooth pasting conditions along the entire threshold boundary $x^\star(t)$, but only at $T^\star$; this is precisely what makes the solution an approximation. In fact, if we attempted to match both V and $\frac{\partial V}{\partial x}$ continuously along the entire threshold $x^*(t)$, we would arrive at a contradiction, which is the reason why this is not an exact solution but an approximation. Since the optimal control depends only on $\frac{\partial V}{\partial x}$, we do not need to need to compute the solution to (30c) for approximating the mean field equilibrium.

Using this quadratic approximation for V, we first solve the Fokker–Planck equation (19) by finite differences, as described below, approximating $\frac{\partial V}{\partial x}$ by $2A_t x + B_t$ in the installation region. Next, we update the mean installation rate via the fixed-point equation (20), which becomes under the quadratic approximation

$$\bar{\nu}_t = \frac{\int_0^{x^\star(t)} (2A_t x + B_t - \alpha)\, m(t,x)\, \mathrm{d}x}{2\beta + \beta N \int_0^{x^\star(t)} m(t,x)\, \mathrm{d}x}, \quad t \in [0,T],$$

and use this updated value to iterate the algorithm until convergence is achieved.

Summary of the algorithm.

1. *Initialization.* Start with an initial guess for $\bar{\nu}$, for example $\bar{\nu}_t = \bar{x}_0(1 - t/T)$.
2. *Mean state dynamics.* Solve numerically $\dot{\bar{x}}_t = -\delta \bar{x}_t + \bar{\nu}_t$ starting from $\bar{x}_0 = x_0$ to obtain the average capacity $\bar{x}_t$.
3. *Non-installation region.* For all t, compute b_t numerically from (27), and use it together with a_t in (28) to determine the threshold $x^\star(t)$. Deduce then $T^\star$ by solving $x^\star(t) = 0$.
4. *Installation region.* Use the quadratic ansatz introduced above where A, B, and C are computed by backward integration from terminal conditions $A_{T^\star} = 0$, $B_{T^\star} = b_{T^\star}$ of the associated ODEs (30).
5. *Fokker–Planck equation.* Starting from the known repartition at time 0, solve forward in time
$$\frac{\partial m}{\partial t} + \frac{\partial}{\partial x}\left[m \left(-\delta x + \frac{(2A_t x + B_t - \alpha - \beta N \bar{\nu}_t)^+}{2\beta} \right) \right] = 0,$$
which corresponds to the FP equation in (19), to obtain the density m. Here we use an explicit Euler finite differences scheme with upwinding for the x derivative.
6. *Update and iterate.* Use the density computed at the previous step in (20) to update $\bar{\nu}$. Return to step 2 with the updated $\bar{\nu}$ and iterate until convergence.

We present a numerical example in which we use the same parameter values as in Section 3.3, see (13), together with $d_1 = 500\$/\text{MWh}$, $d_2 = 10^{-2}\$/\text{MW}^2\text{h}$ specifying the linear price function. For the initial distribution of installed capacities, we consider a truncated exponential distribution. More precisely, we define N discrete capacity levels $x_i = i \cdot \Delta x$ for $i = 1, \ldots, N$, where $\Delta x = x_{\text{end}}/N$ and x_{end} denotes a maximum capacity. We assign exponential weights of the form $w_i = \mathrm{e}^{-Nx_i/X_0}$, which reflect the fact that smaller producers are more common in renewable electricity markets. We then normalize and rescale these weights to define each $x_0^{(i)}$ so that the total initial capacity equals $X_0 = 30\,\text{GW}$. This yields a discrete approximation of a truncated exponential distribution over the grid $\{x_i\}$, with mass concentrated near small capacities and a long tail toward larger producers.

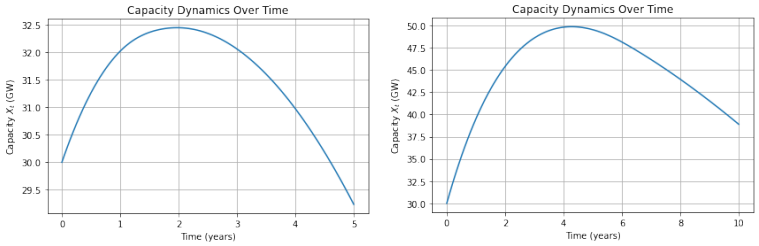

(a) $T = 5$ years (b) $T = 10$ years

Figure 4: Capacity dynamics with linear price function for different time horizons

The resulting capacity trajectories are presented in Figures 4a and 4b, for horizons $T = 5$ and $T = 10$ years, respectively. Based on the numerical computations, we identify the times at which all producers cease installing new capacity: $T^\star \approx 1.71$ in the first case ($T = 5$) and $T^\star \approx 6.26$ in the second ($T = 10$). Beyond these thresholds, no capacity is installed, and the total capacity declines at the natural rate δ.

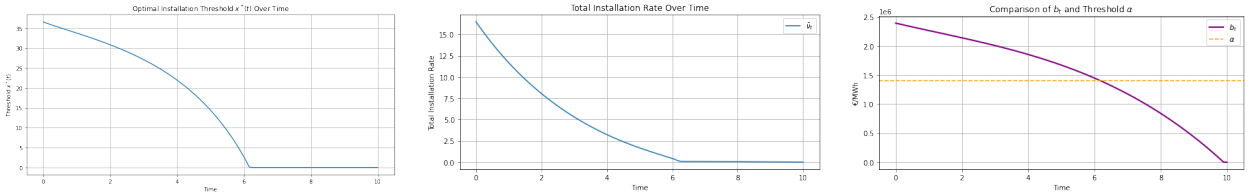

(a) Threshold $x^\star(t)$ (b) Total installation rate K_t (c) Comparison of b_t and α

Figure 5: Threshold between regions and installation rate for $T = 10$ years

For the second case $T = 10$, we also graphically represent in Figure 5a the threshold $x^\star(t)$ between the installation and non-installation regions, and observe that its behavior is similar to the illustration in Figure 3. As shown in Figure 5b, the mean installation rate drops to zero for $t \geq T^\star$, confirming that no capacity is installed beyond this time. Finally, still considering $T = 10$, we also plot in Figure 5c the function b given by (27) in Corollary 4.1. We observe that $b_{T^\star} \approx \alpha$, as expected. Indeed, this follows from the fact that $x^\star(T^\star) = 0$, $\bar{\nu}_{T^\star} = 0$ and the characterization of the threshold curve in (28).

4.3.2 Finite differences method

The other method relies on a classical finite difference scheme. Specifically, we discretize the HJB equation (18) backward in time on a uniform grid over both time and capacity. At each time step, the spatial derivatives $\frac{\partial V}{\partial x}$ are approximated using central differences, which leads to a nonlinear system of equations for the unknown values V_n at the current time layer. This system is then solved using a root-finding algorithm (*e.g.*, `fsolve`).

More precisely, given a uniform grid in time t_n and space x_j with step sizes Δt and Δx, we approximate:

$$\frac{\partial V}{\partial t}(t_n, x_j) \approx \frac{V_j^{n+1} - V_j^n}{\Delta t}, \quad \frac{\partial V}{\partial x}(t_n, x_j) \approx \frac{V_{j+1}^n - V_{j-1}^n}{2\Delta x}.$$

Accordingly, the discretized HJB equation at each grid point (t_n, x_j) takes the form:

$$\frac{V_j^{n+1} - V_j^n}{\Delta t} - rV_j^n - \delta x_j \frac{V_{j+1}^n - V_{j-1}^n}{2\Delta x} + (P(N\bar{x}_n + x_j) - c)hx_j + \frac{1}{4\beta}\left[\left(\frac{V_{j+1}^n - V_{j-1}^n}{2\Delta x} - \alpha - \beta N\bar{\nu}_n\right)^+\right]^2 = 0.$$

At each time step, the system is solved backward in time, using V_{n+1} to compute V_n. We further impose the following boundary conditions at the boundaries of the domain:

- at $x = 0$, we match the value to the solution C_{t_n} obtained by (30c);
- at $x = 0$, we match the value to the solution C_{t_n} obtained by (30c);
- at $x = x_{\max}$, we impose $V_n(x_{\max}) = a_{t_n} x_{\max}^2 + b_{t_n} x_{\max}$;
- at $T = 0$, we impose $V_T^j = 0$.

The results are illustrated in Figure 6 for the following parameters:

$$\begin{aligned} &x_0 = 0.1\text{MW}, \quad c = 1\$/\text{MWh}, \quad r = 0.05\text{year}^{-1}, \quad \delta = \frac{\log 2}{10}\text{year}^{-1}, \quad N = 10, \\ &h = 1\frac{\text{hours}}{\text{year}}, \quad \alpha = 0.1\$/\text{MW}, \quad \frac{1}{2\beta} = 5\text{MW}^2/(\$\text{year}), \quad T = 1 \text{ years}. \end{aligned} \tag{31}$$

The linear price function is further characterized by $d_1 = 2\$/\text{MWh}$ and $d_2 = 1\$/\text{MW}h$.

Figures 6a and 6b display the trajectories of the mean capacity and the optimal control over time. For comparison, we also solve the system numerically using the alternative method that approximates V by two quadratic functions. As shown in Figures 6d and 6e, this approach produces results that are very similar to those obtained with the finite difference scheme. This agreement verifies that both numerical methods are accurate and consistent with each other.

In addition, Figures 6c and 6f show the distribution of capacities at $t = 0$ and $t = 1$. As intended, the initial distribution is exponential, and over time it becomes more concentrated around higher capacities, since producers with smaller initial capacities tend to invest more rapidly.

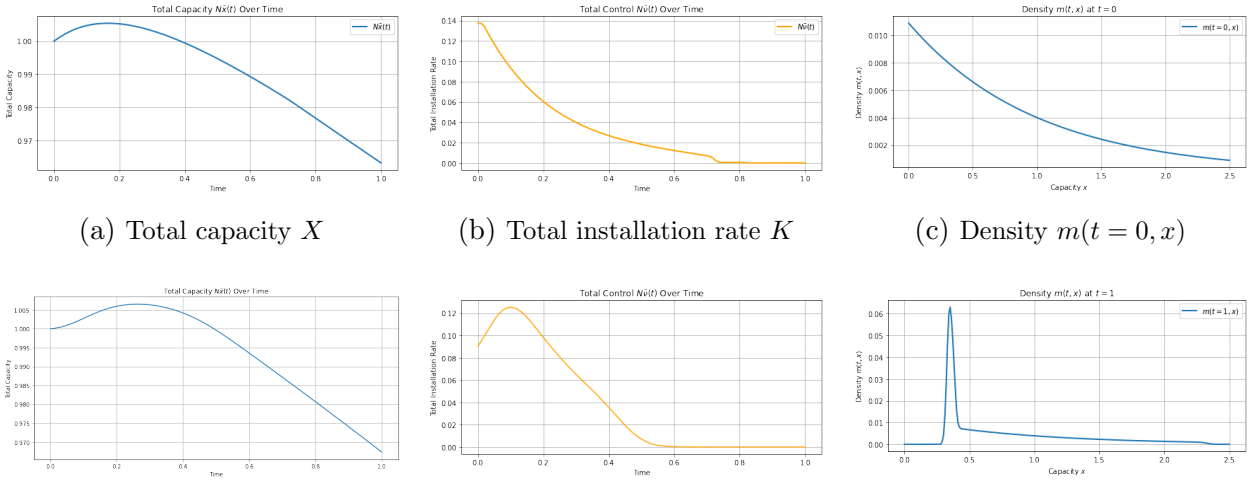

(a) Total capacity X (b) Total installation rate K (c) Density $m(t=0,x)$

(d) X by quadratic approach (e) K by quadratic approach (f) Density $m(t=1,x)$

Figure 6: Simulation results with linear price and parameter values (31)

4.4 Inverse price function

We conclude this section by returning to the inverse price case, examined in [5] and previously in Section 3.3 for the homogeneous case. The main theoretical result presented below directly follows from Proposition 4.1, using the specification $P(x) = p/x$ for the price function.

Corollary 4.2. *In the non-installation region* $\{(t,x) : x \geq x^\star(t)\}$, $V(t,x)$ *is given by*

$$V(t,x) = hx\left(p\int_t^T \frac{\mathrm{e}^{-(r+\delta)(s-t)}}{N\bar{x}_s + x\mathrm{e}^{-\delta(s-t)}}\,\mathrm{d}s - \frac{c}{r+\delta}(1-\mathrm{e}^{-(r+\delta)(T-t)})\right).$$

Therefore, in the non-installation region, we can further compute

$$\frac{\partial V}{\partial x} = h\left(p\int_t^T \frac{\mathrm{e}^{-(r+2\delta)(s-t)}N\bar{x}_s}{(N\bar{x}_s + x\mathrm{e}^{-\delta(s-t)})^2}\,\mathrm{d}s - \frac{c}{r+\delta}(1-\mathrm{e}^{-(r+\delta)(T-t)})\right)$$

which is strictly decreasing in x, confirming that V is indeed concave. Then, $x^\star(t)$ should be determined as the solution, if it exists, to $\frac{\partial V}{\partial x}(t,x^\star(t)) = \alpha + \beta N\,\bar{\nu}_t$, $t \in [0,T]$. However, contrary to the results for the linear price case in Corollary 4.1, no explicit analytic expression for the threshold function can be derived here. Nevertheless, $x^\star(t)$ can be approximated numerically. Moreover, since there is no obvious ansatz to approximate the solution to the HJB equation in the installation region, we focus here on the second numerical method, based on finite differences. Numerical results are presented for the same parameter values used in the previous section, as specified in Equation (31), but with $p = 2\,\$/\mathrm{h}$ to characterize the inverse price function. This value of p is chosen so that the inverse price p/x is of the same order as the linear price $d_1 - d_2 x$ for x near X_0, the initial total capacity, ensuring that the results remain comparable in terms of dynamics and price levels. The trajectories of the mean capacity and the mean installation rate are shown in Figures 7a and 7b respectively.

The simulation shows that the inverse price function $P(x) = \frac{p}{x}$ leads to a strong incentive for early installation: when aggregate capacity $x + N\bar{x}_t$ is low, the electricity price becomes

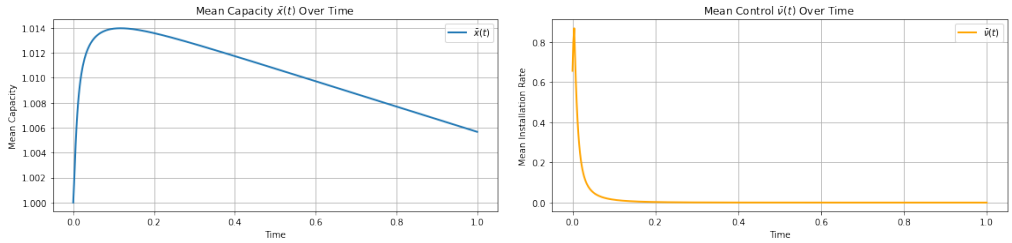

(a) Total capacity $X(t)$ (b) Total installation rate K_t

Figure 7: Simulation results with inverse price and parameter values (31)

very high, resulting in steep marginal rewards for producers. This creates a pronounced front-loading in installation behavior, as producers seek to take advantage of the initially high prices before crowding drives them down. Consequently, total production ramps up sharply in the early part of the horizon.

5 Production intermittency

In this section, we briefly study a version of the model with randomness. Specifically, suppose that x_t evolves according to

$$\mathrm{d}x_t = (-\delta x_t + \nu_t)\mathrm{d}t + \sigma x_t \mathrm{d}W_t, \quad t \in [0, T],$$

where W is a Brownian Motion. Introducing randomness in the installed capacity x_t indirectly generates volatility in the instantaneous profit $hx_t(P(X_t) - c)$. In this sense, incorporating stochastic fluctuations in the state variable x_t could serve to model the intermittency of renewable energy sources—such as variations in solar or wind output—which leads to uncertain revenue streams. The variability from intermittency of renewables (see, for instance Carmona and Yang (2024) [11]) increases the sensitivity of grids to fluctuations. Large-scale expansions, without corresponding flexibility measures, can make systems more exposed to operational risks (see Shrivats, Sircar, and Yang (2024) [28]).

The value function should now be defined as follows,

$$V(t,x) = \sup_{\nu \geq 0} \mathbb{E}\left[\int_t^T \mathrm{e}^{-r(s-t)} \left(h(P(x_s + N\bar{x}_s) - c)x_s - \nu_s(\alpha + \beta(\nu_s + N\bar{\nu}_s))\right) \mathrm{d}s \,\middle|\, x_t = x\right],$$

for all $(t,x) \in [0,T] \times \mathbb{R}$. The form of the optimal control remains the same as (17), and the corresponding HJB equation is similar to (18),

$$\frac{\partial V}{\partial t} - rV - \delta x \frac{\partial V}{\partial x} + hx(P(x + \bar{x}_t N) - c) + \frac{[(\frac{\partial V}{\partial x} - \alpha - \beta N \bar{\nu}_t)^+]^2}{4\beta} + \frac{1}{2}\sigma^2 x^2 \frac{\partial^2 V}{\partial x^2} = 0,$$

with terminal condition $V(T,x) = 0$. More precisely, if we let $\sigma = 0$ in the above HJB equation, we recover (18). Similarly, the Fokker-Planck becomes

$$\frac{\partial}{\partial t} m + \frac{\partial}{\partial x}\left[m\left(-\delta x + \frac{(\frac{\partial V}{\partial x} - \alpha - \beta N \bar{\nu}_t)^+}{2\beta}\right)\right] = \frac{1}{2}\frac{\partial^2}{\partial x^2}\left(\sigma^2 x^2 m\right).$$

Finally, the fixed point condition coincides with (20). Intuitively, this model is expected to yield outcomes that closely resemble those of the deterministic setting studied in the previous sections. For conciseness, we limit ourselves in this section to presenting a numerical example that illustrates this resemblance. Specifically, when the price is linear and $\sigma^2 < r + 2\delta$, the two numerical methods described earlier can be implemented.

The analogue of the first method discussed in Section 4.3.1 is to approximate V by a quadratic function in each of the two regions, namely

$$V(t,x) = \begin{cases} A_t x^2 + B_t x + C_t, & \text{if } \frac{\partial V}{\partial x}(t,x) \geq \alpha + \beta N \bar{\nu}_t \\ a_t x^2 + b_t x, & \text{if } \frac{\partial V}{\partial x}(t,x) < \alpha + \beta N \bar{\nu}_t, \end{cases}$$

with b, B, C solutions to the same equations (27, 30b, 30c) as before, but a, A now solve

$$\dot{a}_t = (r + 2\delta - \sigma^2)a_t + hd_2, \quad \dot{A}_t = (r + 2\delta - \sigma^2)A_t + hd_2 - \frac{A_t^2}{\beta}.$$

Then, we can apply the numerical method of Section 4.3.1 and solve these two equations.

Alternatively, we can directly discretize the HJB equation using a central finite difference scheme, following the approach described in Section 4.3.2. The resulting discretized HJB equation takes the form

$$\begin{aligned} &\frac{V_j^{n+1} - V_j^n}{\Delta t} - rV_j^n - \delta x_j \frac{V_{j+1}^n - V_{j-1}^n}{2\Delta x} + (P(N\bar{x}_n + x_j) - c)hx_j \\ &+ \frac{1}{4\beta}\left[\left(\frac{V_{j+1}^n - V_{j-1}^n}{2\Delta x} - \alpha - \beta N \bar{\nu}_n\right)^+\right]^2 + \frac{\sigma^2 x_j^2}{2} \frac{V_{j+1}^n - 2V_j^n + V_{j-1}^n}{(\Delta x)^2} = 0. \end{aligned}$$

For illustration, we apply the first method with the same parameters as in Section 4.3.1, with $T = 10$ and $\sigma = 0.4$. The resulting capacity is shown in Figure 8a, and the threshold $x^\star(t)$ is presented in Figure 8b. We observe that the capacity trajectory with randomness (orange dotted curve) closely resembles the deterministic trajectory (blue curve). However, $x^\star(t)$ is noticeably smaller compared to Figure 5a. This difference arises because a_t becomes much larger when $\sigma > 0$, since $(r + 2\delta - \sigma^2) < (r + 2\delta)$.

This reduction reflects agents' increased caution under uncertainty. In particular, the stochastic component in the dynamics introduces a precautionary effect, where firms may delay or reduce investments to hedge against downside risks. This behavior is consistent with real-world observations, where firms facing high uncertainty (*e.g.*, due to variable output from renewables or policy instability) often exhibit more conservative expansion strategies.

6 Conclusion

We conclude with a few modeling comments that suggest possible extensions or refinements of the current setup.

While we model the electricity price as a function of total installed capacity only, a more general formulation could allow the price to depend explicitly on time, *i.e.* $P = P(t, X_t)$, to

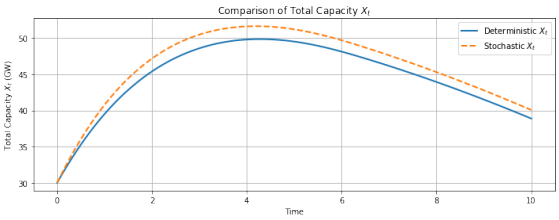

(a) Total capacity X_t

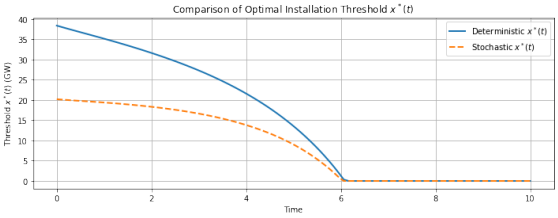

(b) Threshold $x^\star(t)$

Figure 8: Capacity dynamics and threshold for linear price function and $T = 10$

capture external seasonal effects, regulatory interventions, or trends in demand that are not driven solely by supply. Incorporating such time dependence could be particularly relevant for settings where electricity prices exhibit strong periodic or structural trends.

Another possible extension is to introduce heterogeneity across firms in terms of cost structures, risk preferences, or technologies. For instance, the marginal installation cost α could be modeled as a decreasing function of installed capacity x, reflecting economies of scale. Similarly, the crowding sensitivity parameter β could also be specified as $\beta(x)$, decreasing in x, to capture the idea that larger firms may face lower relative frictions due to better access to contractors, permits, or supply chains. This would allow larger producers to install capacity more efficiently than smaller ones, capturing realistic differences in incentives between incumbents and new entrants.

Taking into account storage investment decisions and flexible resources (*e.g.* demand response, dispatchable backup) into the model would allow to assess their interaction with intermittent renewable deployment. Recent events—such as the major power outage in Spain and Portugal triggered by grid imbalances and a lack of short-term flexibility [6]—highlight the critical role of these mechanisms in ensuring system stability during high-renewable penetration.

Finally, it could be relevant to study the impact of various policy tools—such as carbon taxes, renewable subsidies, or capacity remuneration mechanisms—on long-term investment decisions within the mean field framework. For instance, as in [5], one could model subsidies that reduce the marginal cost of production c or the installation cost α, and examine how these interventions shift the equilibrium and accelerate renewable deployment.

References

[1] R. Aïd, L. Campi, A. Nguyen Huu, and N. Touzi. A structural risk–neutral model of electricity prices. *International Journal of Theoretical and Applied Finance*, 12(7): 925–947, 2009.

[2] R. Aïd, R. Dumitrescu, and P. Tankov. The entry and exit game in the electricity

markets: a mean-field game approach. *Journal of Dynamics and Games*, 8(4):331–358, 2021.

[3] R. Aïd, S. Federico, G. Ferrari, and N. Rodosthenous. Regulation in a mean-field investment game with climate damage. *Preprint SSRN 5235340*, 2025.

[4] C. Alasseur, I. Ben Taher, and A. Matoussi. An extended mean field game for storage in smart grids. *Journal of Optimization Theory and Applications*, 184(2):644–670, 2020.

[5] C. Alasseur, M. Basei, C. Bertucci, and A. Cecchin. A mean field model for the development of renewable capacities. *Mathematics and Financial Economics*, 17(4):695–719, 2023.

[6] R. Bajo-Buenestado. The Iberian Peninsula blackout — Causes, consequences, and challenges ahead. Technical report, Rice University's Baker Institute for Public Policy, 2025.

[7] A. Bassière, R. Dumitrescu, and P. Tankov. A mean-field game model of electricity market dynamics. In F. E. Benth and A. E. D. Veraart, editors, *Quantitative Energy Finance: Recent Trends and Developments*, pages 181–219. Springer Nature Switzerland, 2024.

[8] M. Bichuch, G. Dayanıklı, and M. Lauriere. A stackelberg mean field game for green regulator with a large number of prosumers. *Preprint SSRN 4985557*, 2024.

[9] D. Cacciarelli, P. Pinson, F. Panagiotopoulos, D. Dixon, and L. Blaxland. Do we actually understand the impact of renewables on electricity prices? A causal inference approach. *Preprint arXiv:2501.10423*, 2025.

[10] R. Carmona and M. Ludkovski. Valuation of energy storage: an optimal switching approach. *Quantitative Finance*, 10(4):359–374, 2010.

[11] R. Carmona and X. Yang. Joint granular model for load, solar and wind power scenario generation. *IEEE Transactions on Sustainable Energy*, 15(1):674–686, 2024.

[12] R. Carmona and C. Zeng. Leveraging the turnpike effect for mean field games numerics. *IEEE Open Journal of Control Systems*, 3:389–404, 2024.

[13] R. Carmona, G. Dayanıklı, and M. Laurière. Mean field models to regulate carbon emissions in electricity production. *Dynamic Games and Applications*, 12(3):897–928, 2022.

[14] R. Carmona, G. Dayanikli, F. Delarue, and M. Lauriere. From Nash equilibrium to social optimum and vice versa: a mean field perspective. *Preprint arXiv:2312.10526*, 2023.

[15] P. Chan and R. Sircar. Fracking, renewables, and mean field games. *SIAM Review*, 59 (3):588–615, 2017.

[16] G. Dayanikli and M. Laurière. Multi-population mean field games with multiple major players: application to carbon emission regulations. In *2024 American Control Conference*, pages 5075–5081, 2024.

[17] G. Dayanikli and M. Lauriere. Cooperation, competition, and common pool resources in mean field games. *Preprint arXiv:2504.09043*, 2025.

[18] R. Dumitrescu, M. Leutscher, and P. Tankov. Energy transition under scenario uncertainty: a mean-field game of stopping with common noise. *Mathematics and Financial Economics*, 18(2):233–274, 2024.

[19] R. Élie, E. Hubert, T. Mastrolia, and D. Possamaï. Mean-field moral hazard for optimal energy demand response management. *Mathematical Finance*, 31(1):399–473, 2021.

[20] C. Escribe, J. Garnier, and E. Gobet. A mean field game model for renewable investment under long-term uncertainty and risk aversion. *Dynamic Games and Applications*, 14 (5):1093–1130, 2024.

[21] D. Firoozi, A. V. Shrivats, and S. Jaimungal. Principal agent mean field games in REC markets. *Preprint arXiv:2112.11963*, 2022.

[22] N. Garcia, M. Reppen, and R. Sircar. Continuum aggregate games. *In preparation*, 2025.

[23] N. Garcia, R. Sircar, and M. Soner. Mean field games of control and cryptocurrency mining. *Preprint*, 2025.

[24] O. Guéant, J.-M. Lasry, and P.-L. Lions. Mean field games and applications. In *Paris-Princeton Lectures on Mathematical Finance 2010*, volume 2003, pages 205–266. Springer Berlin Heidelberg, Berlin, Heidelberg, 2011.

[25] N. Hernández Santibáñez, A. Jofré, and D. Possamaï. Pollution regulation for electricity generators in a transmission network. *SIAM Journal on Control and Optimization*, 61 (2):788–819, 2023.

[26] Z. Li, A. M. Reppen, and R. Sircar. A mean field games model for cryptocurrency mining. *Management Science*, 70(4):2188–2208, 2024.

[27] M. Ludkovski and R. Sircar. Technology ladders and R&D in dynamic Cournot markets. *Journal of Economic Dynamics and Control*, 69:127–151, 2016.

[28] A. Shrivats, R. Sircar, and X. Yang. Quantifying renewables reliability risk in modern and future electric grids. *The Journal of Energy Markets*, 2024. To appear.